

1 Data Descriptor Template

Scope Guidelines

Data Descriptors submitted to *Scientific Data* should provide detailed descriptions of valuable research datasets, including the methods used to collect the data and technical analyses supporting the quality of the measurements. Data Descriptors focus on helping others reuse data, rather than testing hypotheses, or presenting new interpretations, methods or in-depth analyses. Relevant datasets must be deposited in an appropriate public repository prior to Data Descriptor submission, and their completeness will be considered during editorial evaluation and peer review. The data must be made publicly available without restriction in the event that the Data Descriptor is accepted for publication (excepting reasonable controls related to human privacy issues or public safety).

2

3 Title

4 Three-dimensional reconstruction of high latitude bamboo coral via X-ray microfocus
5 Computed Tomography

6

7 Authors

8 Thomas J Williams^{1*}, Philip J. Basford², Orestis L. Katsamenis², Martin Solan¹, Gavin L. Foster¹,
9 Christopher Standish¹, Jasmin A. Godbold¹, Philippe Archambault³

10

11 Affiliations

12 1. School of Ocean and Earth Science, National Oceanography Centre Southampton, University
13 of Southampton, Waterfront Campus, European Way, Southampton SO14 3ZH, UK

14 2. μ -VIS X-ray Imaging Centre, Building 5, University of Southampton, Highfield Campus,
15 University Road, Southampton, SO17 1BJ, UK

16 3. ArcticNet, Québec Océan, Takuvik Joint International Laboratory CNRS, Université Laval,
17 Québec City, QC, Canada

18

19 * corresponding author(s): Thomas J Williams (T.Williams@soton.ac.uk)

20

21 Abstract

22 The skeletons of long-lived bamboo coral (Family *Keratoisididae*) are promising archives for
23 deep-water palaeoceanographic reconstructions as they can record environmental variation
24 at sub-decadal resolution in locations where *in-situ* measurements lack temporal coverage.
25 Yet, detailed three dimensional (3D) characterisations of bamboo coral skeletal architecture
26 are not routinely available and non-destructive investigations into microscale variations in
27 calcification are rare. Here, we provide high-resolution micro-focus computed tomography
28 (μ CT) data of skeletal density for two species of bamboo coral (*Acanella arbuscula*: 5
29 specimens, voxel size, 15 μ m (central branch scans) and 50 μ m (complete structure scan);
30 *Keratoisis* sp.: 4 specimens, voxel size, 15 μ m) collected from the Labrador Sea and Baffin Bay
31 deep-water basins. These data provide reference models useful for developing methods to
32 assess structural integrity and other fine-scale complexities in many biological, geological, and
33 industrial systems. This will be of wider value to those investigating structural composition,

34 arrangement and/or composition of complex architecture within the fields and subdisciplines
35 of biology, ecology, medicine, environmental geology, and structural engineering.
36

37 **Background & Summary**

38 Deep-water bamboo corals form complex structures that, as they grow, archive seasonally
39 resolved oceanographic information¹. This information is important for efforts to reconstruct
40 both recent and ancient environmental conditions². Stands of these corals also play an
41 important role in mediating benthic biodiversity and functioning by enhancing the density of
42 bioturbators and sediment nutrient release³, but a combination of their extended longevity
43 (>100 years⁴) and slow growth rates⁵ mean that populations are vulnerable to physical
44 disturbance⁶ such that intact specimens have seldom been sampled and are not widely
45 available. Yet, detailed information on coral skeletal architecture is vital for understanding
46 calcification strategies and growth patterns⁷ in response to changing environmental
47 circumstance, and can be informative for marine planning and conservation measures⁸.

48
49 Techniques used to investigate the microstructure of coral skeletons, such as scanning
50 electron microscopy (SEM) and grinding sections, have relied on methods that require high
51 workloads, strict operability and destructive preparation work⁹. Recent imaging methods, such
52 as high-resolution micro-focus computed tomography (μ CT), removes these constraints and,
53 as it allows quantitative analyses of coral skeletal microarchitecture, is emerging as a growing
54 area of scientific focus¹⁰⁻¹¹ for contemporary investigations of reef-building coral skeletons¹²⁻
55 ¹⁶.

56
57 This data descriptor presents μ CT scans of two species of deep-water bamboo coral (*Acanella*
58 *arbuscula* and *Keratoisis* sp.) obtained from the Eastern Canadian Arctic. These μ CT scans can
59 provide reference models which may be of use in the development of novel structural designs,
60 analysis routines and computer models for fields such as ecology¹⁷ orthopaedics¹⁸,
61 environmental geology and structural engineering¹⁹. The data may also be of particular
62 interest to those investigating radial growth patterns and banding²⁰, coral calcification and
63 bioerosion²¹, impacts of climate change on marine calcifiers²²⁻²³, coral skeletal-canal
64 networks²⁴ and coral-to-bone substitute biocompatibility²⁵. The data files are provided as a
65 sequence of stacked tagged image file format (TIFF) images for each scan. These tiff stacks can
66 be opened by a variety of software, including Fiji/ImageJ, which includes instructions for
67 opening in the accompanying user manual²⁶.

68

69 **Methods**

70 Five specimens of *Acanella arbuscula* and four specimens of *Keratoisis* sp. were collected from
71 two deep-water stations (Davis Strait; 63° 20.7198' N; 58° 11.7426' W, 1311 m, 3.5 °C, 34.9
72 psu, 29th July 2021, Disko Fan; 67° 57.9786' N, 59° 29.6286' W, 889 m, 1.1 °C, 33.5 psu, 2nd
73 August 2021) using a remotely operated submersible (Sub-Atlantic® Comanche, Forum Energy
74 Technologies™, USA) during the 2021 Amundsen expedition (15th July 2021 – 12th August 2021
75 onboard the *CCGS Amundsen*). These stations reside within the historically heavily fished²⁷,
76 and now Marine Conservation Areas (since 2017²⁸⁻²⁹), of the Eastern Canadian Arctic. Permits

77 to Fish for Scientific Purposes were obtained from Fisheries and Oceans Canada (Licence NL-
78 6515-21; Licence S-21/22-1030-NU). *A. arbuscula* is considered an indicator of Vulnerable
79 Marine Ecosystems³⁰ whilst *Keratoisis* sp. has not, to date, been found anywhere else in the
80 world³¹. Where possible, the corals were sampled at or close to the basal internode (near the
81 base of the specimen at the sediment surface). Any external debris and residing fauna were
82 carefully removed from the collected colonies using tweezers before each specimen was
83 sealed in a plastic Ziplock bag and frozen at -20 °C. After 72 hours, the specimens were
84 removed from the freezer and carefully cleaned with jets of re-circulated 0.45 µm membrane-
85 filtered seawater (FSW) at 4 °C using a WaterPik™ before being placed back in -20 °C³². The
86 cleaned skeleton portions were then sealed in new Ziplock plastic sample bags enclosed in
87 Tupperware (*Acanella arbuscula*) or PVC vinyl tubing (*Keratoisis* sp.) before being transported
88 to the University of Southampton, UK. Here, the specimens were re-housed within Perspex
89 tubes, sealed with polystyrene bungs (Figure 1), and brought to the µ-VIS X-ray Imaging Centre
90 (www.muvis.org) for µCT scanning. Specifically, imaging took place at the centre's 3D X-ray
91 Histology (XRH) facility at the University Hospital Southampton³³, which is the centre's
92 dedicated division for biomedical imaging.

93
94 Reconstruction of biogenic structures was achieved using a custom designed Nikon XT micro-
95 focus computed tomography housed within the 3D X-ray Histology (XRH) facility. This system
96 is based on the XT H 225 ST (Nikon Tring, UK). As the system used to acquire the scan data
97 requires the corals to be held vertically, specimens were secured upright in custom-made
98 Perspex holding tubes with polystyrene bungs to ensure stability and prevent movement
99 during rotation (360 degrees) and scanning (Figure 1). The scans (acquisition time: 15 – 83
100 minutes; total projections: 2001 – 3501) were all performed at 80 KVP using a Molybdenum
101 target with no filtration. The detector in the scanner is 2850x2850 pixels and was used un-
102 binned. For the overview scans of *A. arbuscula* at 50 µm a 12 W power could be used, however,
103 for the higher resolution scans (15 µm; *A. arbuscula* and *Keratoisis* sp.) this was reduced to 6.9
104 W to allow for a sharper (smaller) X-ray focal spot (see Table 1 for more scan parameters).
105 Additionally, a tube of water was scanned at the same time as the samples under the same
106 beam conditions to allow it to be used as a density phantom. The work this data was collected
107 to support focuses on studying the phenotype (microanatomy), which does not require
108 densitometric calibration. However, it was recognised that this may be valuable in the future
109 so the raw data required to calibrate the scans was collected at the same time for
110 futureproofing the datasets. As of now, the data-size limitations set by repositories dictate
111 that access to these raw data files can only be obtained by reaching out to the authors. All
112 reconstructions were performed using CT Pro 3D 6.6 or 6.7 (Nikon Xtek, Tring UK). The
113 reconstructions were performed using Nikon CT Pro/CT Agent with the beam hardening 4
114 preset. The software performs a linearisation operation of the beam hardening curves using a
115 pre-determined correction profile. Preset 4 uses the following variables: CoefX4=0.0,
116 CoefX3=0.0, CoefX2=0.8, CoefX1=0.2, CoefX0=0.0, Scale=4.44. No additional ring filter or noise
117 filter was specified.

118 The field of view for the desired resolution did not allow the full height of the *Keratoisis*
119 samples (11.1 – 24.5 cm) to be scanned in a single scan, so multiple overlapping vertical scan
120 positions (n = 3) were used which were then concatenated after reconstruction. The chosen
121 overlap was designed specifically to exclude cone-beam under-sampling artifacts that occur at

122 the top and bottom of the reconstructed space from the concatenated volume. The
123 concatenation was performed using a custom written macro for Fiji titled
124 'AutomaticConcatenationPlusIntensityEqualisation' from the XRH toolbox³⁴, which enables
125 the user to manually or automatically select the fusion slice on each volume. If textural
126 information is sufficient and variation from slice to slice significant, the selection can be done
127 automatically. If not, user can select to bypass the automatic slice selection and select the
128 fusion slice manually. The script then crops the bottom volume between "slice one" and up to
129 the "selected slice", and top volume from "selected slice" up to "last slice", and before
130 stitching them into a single volume adjusts the contrast and brightness of the first image of
131 the top volume to match that of the last image of the bottom volume. This ensures a "smooth"
132 transition from one volume to the other and corrects the intensity variations caused by the
133 heel effect. Intensity calibration is carried out by sampling regions of interest (ROIs) and fitting
134 a straight line using mean intensity values. The parameters obtained from the calibration are
135 applied to the "top" stack to linearly shift the intensity window of the top volume. The two
136 stacks are subsequently concatenated into a single stack and a preview of the concatenated
137 stack is generated by performing a radial reslice to allow the user to evaluate the
138 "smoothness" of the transition. The process can then be repeated to concatenate a third
139 volume onto of the resulted volume-1 + volume-2 volume, etc. Following concatenation on
140 the 32-bit, the resulted volume it was converted to 8-bit in Fiji/ImageJ (v 1.53c²⁶) to reduce
141 the data size making it easier to process. These complete volumes were then exported as tiff
142 stacks to enable upload into the Polar Data Centre³⁵, as such, the macro does not need to be
143 run a second time on the data files.

144

145 In the stacked images (Figure 2) and three-dimensional volumes (Figure 3), levels of grey scale
146 reflect the level of X-ray attenuation caused by variation in bulk density. In this case, brighter
147 pixels represent denser material (calcium carbonate) with darker pixels representing less
148 dense material (organic tissue). To refine coral visualisations, the three-dimensional image
149 captured of the holding tube can be discarded during image processing to leave the skeletal
150 volume (Figure 3).

151

152 **Data Records**

153 All data records (in addition to information regarding data structure, file names, and folder
154 structure) listed in this section are available at the Polar Data Centre³⁵. To override the default
155 maximum number of displayed files (n = 1000) in each sub-directory, add the following string
156 "&max=N" to the end of the repository URL, where "N" is the number of files you would like
157 to access. Computed tomography three-dimensional 8-bit volumes have been converted to
158 stacked tagged image file format (TIFF) images with associated dimension data (image width,
159 image breadth, stack height) and scan information presented in portable document format
160 reports (pdfs) to enable access by multiple processing programs. There are five sets of images
161 for *A. arbuscula* complete structure (n = 5), five sets of images for *A. arbuscula* central branch
162 (n = 5) and 4 sets of images for *Keratoisis* sp. (n = 4).

163

164 **Technical Validation**

165 **μ-CT calibration**

166 Regular quality assurance inspections are carried out on the μ-CT scanner to verify its
167 metrological and geometrical (alignments) accuracy for conducting the scans. The geometry
168 of source to object and source to detector distances are verified whenever there is any
169 significant physical interaction with the source such as re-alignment, change of filament, or
170 source anode change. This calibration process involves scanning a specially designed phantom
171 known as an 'hourglass'³⁶, which consists of three pairs of high-sphericity spheres. The sphere
172 sizes are as follows: two spheres with a diameter of 3.000 mm, two spheres with a diameter
173 of 6.000 mm, and two spheres with a diameter of 9.525 mm, and each sphere is kept in contact
174 with its size-counterpart. By using this phantom, it becomes possible to accurately determine
175 a known distance, specifically the centre-to-centre distance of the spheres, in a threshold-
176 independent manner. If the measured distance deviates beyond the acceptable limits of
177 metrological accuracy, the system's calibration parameters are adjusted to ensure agreement
178 between the measured distance and the actual distance.

179

180 **Usage Notes**

181 The software options suitable for analysing the data files range from open-source suites, such
182 as Fiji/ImageJ²⁶, ITK Snap³⁷ or HOROS[®] (The Horos Project) to commercial software suites such
183 as VGSTUDIO MAX (Volume Graphics), Avizo[®] (Thermo Fisher Scientific), Simpleware
184 (Synopsys Inc), OsyriX[®] (Pixmeo), or Dragonfly (Object Research Systems). For instructions on
185 how to open the files please refer to the user manual of the software chosen. The toolbox
186 containing the "Automatic Concatenation Plus Intensity Equalisation" has a file which
187 summarises the functionality of each script and gives an overview of the options available for
188 each script³⁴.

189

190 **Code Availability**

191 *The code used for the concatenation of scans is available as part of the XRH toolbox at*
192 <https://doi.org/10.5281/zenodo.11148752>³⁴.

193 **Concatenation code description**

194 A high-level overview of the custom concatenation code is given below. This can be used as
195 template to reproduce the code in any language the reader is more familiar with.

196

197 **Start**

- 198 1. Prompt user to select the "BOTTOM" stack and store its title and bit depth.
- 199 2. Prompt user to select the "TOP" stack and store its title and bit depth.
- 200 3. Set measurements for analysis.
- 201 4. Create a dialog box to configure options.
- 202 5. Retrieve selected options from the dialog box.
- 203 6. If bit depths are different, display error message and exit.
- 204 7. If manual XY translation option is selected:
 - 205 a. Set the measurement tool to a point.
 - 206 b. Prompt the user to select a point of alignment in the "btm" stack
207 and measure its coordinates.

- 208 c. Prompt the user to select a point of alignment in the "top" stack
- 209 and measure its coordinates.
- 210 d. Calculate the translation values and convert them to pixel units.
- 211 e. Translate the "top" stack using the calculated translation values.
- 212 8. If **automatic slice selection** option is selected:
- 213 a. Prompt user to navigate to fusion point in "btm" stack.
- 214 b. Create reference image from selected slice.
- 215 c. Normalize reference image.
- 216 d. Normalize each slice in "top" stack.
- 217 e. Subtract reference image from "top" stack.
- 218 f. Calculate standard deviation for each slice.
- 219 g. Find slice with minimum standard deviation.
- 220 9. If **manual slice selection** option is selected:
- 221 a. Prompt user to navigate to fusion point on both "top" and "bottom"
- 222 volumes and retrieve the slice numbers.
- 223 10. Create duplicates of "btm" and "top" stacks by cropping btm volume between "slice
- 224 1" up to the "selected slice", and "top" volume from "selected slice" up to "last slice"
- 225 11. Perform intensity calibration by sampling ROIs and fitting a straight line.
- 226 12. Apply intensity calibration parameters to "top" stack.
- 227 13. Concatenate cropped "btm" and cropped & calibrated "top" stacks into single stack.
- 228 14. Perform preview concatenation by creating radial reslice.
- 229 **End**
- 230

231 **Acknowledgements**

232 Supported by a National Environmental Research Council Funded (INSPIRE) PhD [grant number
233 NE/S007210/1, 2019-2027, awarded to T.J.W], the National Research Facility for Lab X-ray CT
234 (NXCT) [EPSRC grant number EP/T02593X/1], the European Research Council Advanced Grant
235 Microns2Reefs [grant agreement ID 884650, awarded to G.L.F.] and a grant from NVIDIA
236 [utilized an NVIDIA RTX A6000]. For the purpose of open access, the author has applied a CC
237 BY public copyright licence to any Author Accepted Manuscript version arising from this
238 submission. We acknowledge the Université Laval for additional support that allowed
239 participation in the 2021 Amundsen expedition onboard the Canadian research icebreaker
240 CCGS Amundsen. We thank Keith Tamburri (CSSF-ROPOS), Peter Lockhart (CSSF-ROPOS), Barry
241 Brake (CSSF-ROPOS), Dr. Evan Edinger (Memorial University of Newfoundland), Dr. Bárbara de
242 Moura Neves (Fisheries and Oceans Canada) and Guillaume Blais (Université Laval) for
243 assisting in the collection and processing of the coral specimens. We thank the scientific
244 personnel and crew of the 2021 Amundsen expedition, and the Amundsen Science Inc. team,
245 which is supported by the Canada Foundation for Innovation, for their assistance and logistical
246 support leading up to, during and after the expedition. The views expressed in this publication
247 do not necessarily represent the views of Amundsen Science or that of its partners.

248

249 **Author contributions**

250 T.J.W. participated in the 2021 Amundsen expedition and collected, processed and
251 transported the corals to the University of Southampton for μ CT. P.J.B. and O.L.K. developed
252 the imaging protocol and acquired the three-dimensional coral volumes using μ CT. T.J.W.
253 processed the coral volumes with assistance from O.L.K. and P.J.B. T.J.W. and M.S. prepared

254 the manuscript. P.J.B. and O.L.K. provided details on methods and technical validation. All
255 authors provided input on the manuscript.

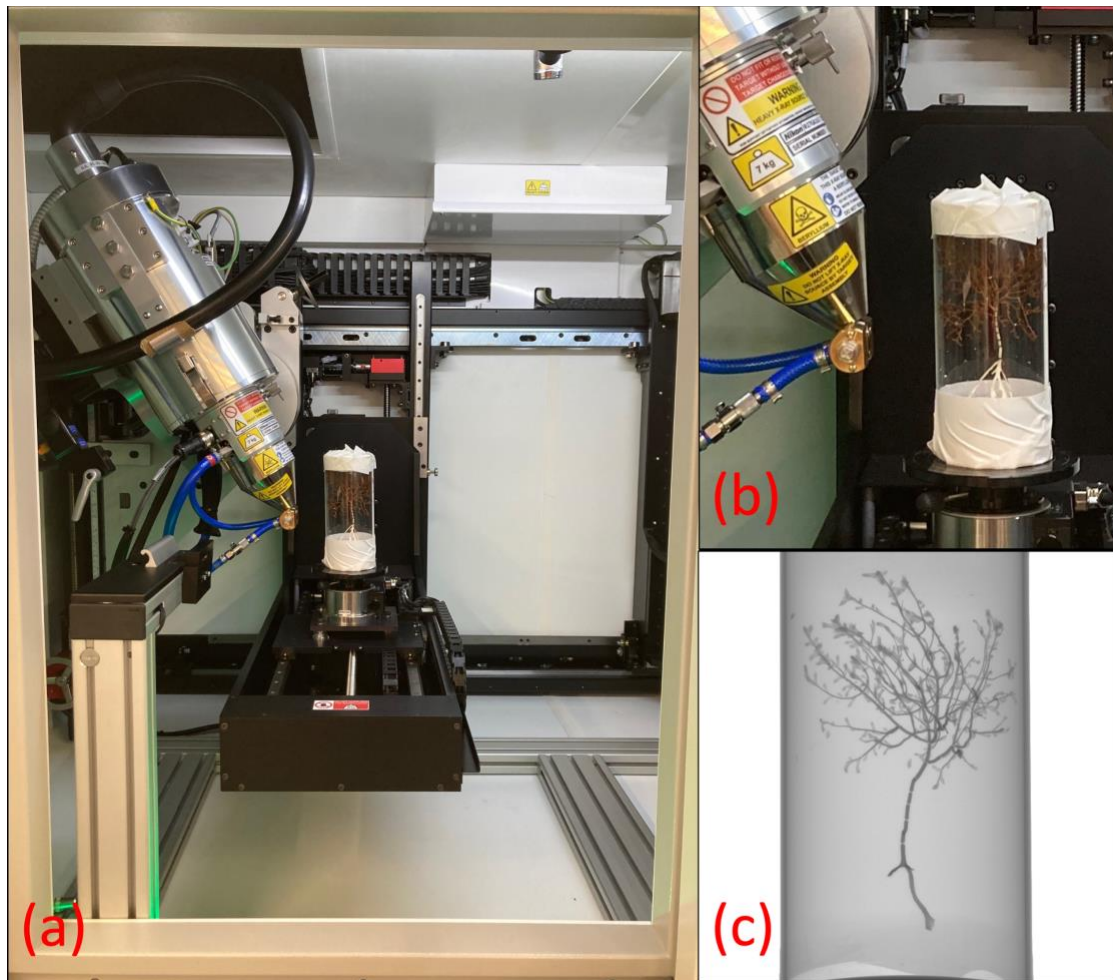
256 **Competing interests**

257 The authors declare there are no competing interests.

258 **Figures**

259

260 Figure 1.



261

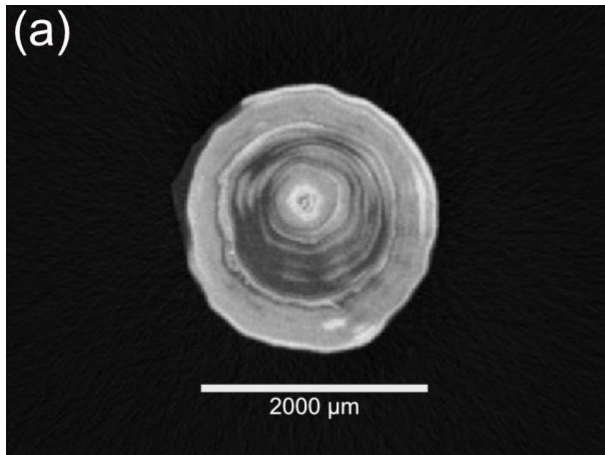
262 Figure 1. (a) Overview, (b) Close-up and (c) Radiograph of an *Acanella arbuscula* specimen

263 inside a Perspex holding tube in the micro-focus computed tomography scanner housed

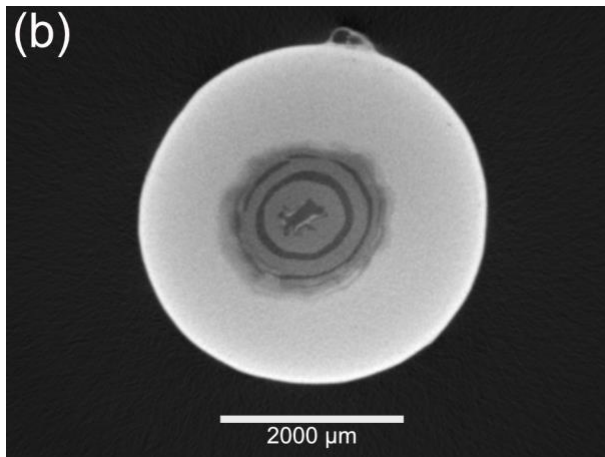
264 within the 3D X-ray Histology (XRH) Biomedical Imaging Unit facility at University Hospital

265 Southampton.

266 Figure 2.
267 (a)



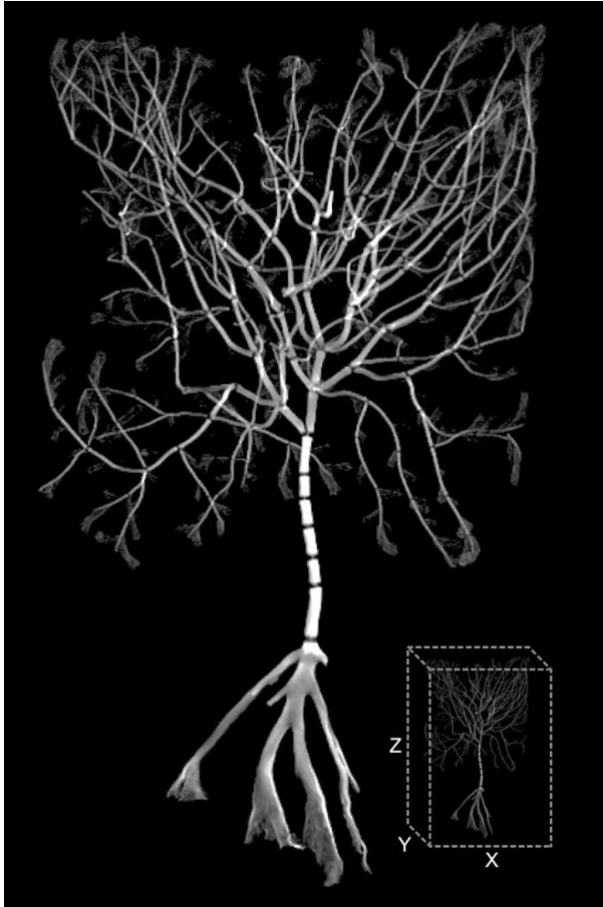
268
269
270 (b)



271
272
273
274
275
276
277

Figure 2. A scaled transverse slice (voxel size, 15 μm) from the (a) *Acanella arbuscula* 8-bit coral volumes image set and (b) *Keratoisis* sp. 8-bit coral volumes image set showing rings of low density organic tissue (dark grey) and higher density calcium carbonate (light grey) at the node-internode connection, viewed in Fiji²⁶ (v2.3.0). Each coral volume image set consists of numbered images that are sequentially stacked to create the three-dimensional coral model.

278 Figure 3.



279
280
281
282
283
284

Figure 3. Representative example of reconstructed three-dimensional coral model for *Acanella arbuscula* created from the stacked 8-bit coral volumes images in Dragonfly (v2022.1); approximate dimensions 89 x 85 x 142 (XYZ) mm.

285 **Figure Legends**

286

287 Figure 1. (a) Overview, (b) Close-up and (c) Radiograph of an *Acanella arbuscula* specimen
288 inside a Perspex holding tube in the micro-focus computed tomography scanner housed
289 within the 3D X-ray Histology (XRH) Biomedical Imaging Unit facility at University Hospital
290 Southampton.

291

292 Figure 2. A scaled transverse slice (voxel size, 15 μm) from the (a) *Acanella arbuscula* 8-bit
293 coral volumes image set and (b) *Keratoisis* sp. 8-bit coral volumes image set showing rings of
294 low density organic tissue (dark grey) and higher density calcium carbonate (light grey) at the
295 node-internode connection, viewed in Fiji²⁶ (v2.3.0). Each coral volume image set consists of
296 numbered images that are sequentially stacked to create the three-dimensional coral model.

297

298 Figure 3. Representative example of reconstructed three-dimensional coral model for *Acanella*
299 *arbuscula* created from the stacked 8-bit coral volumes images in Dragonfly (v2022.1);
300 approximate dimensions 89 x 85 x 142 (XYZ) mm.

301

302 **Tables**

303

304 Table 1. Typical operating parameters during scans of *Acanella arbuscula* and *Keratoisis* sp.
 305 specimens in the custom designed Nikon XT micro-focus computed tomography housed
 306 within the 3D X-ray Histology (XRH) facility.

307

308

<i>Species</i>	<i>Scan type</i>	<i>Acquisition mode</i>	<i>Isotropic voxel edge size (μm)</i>	<i>Isotropic voxel edge size (μm)</i>	<i>Beam Energy (KVp)</i>	<i>X-ray Power (W)</i>	<i>Number of projections</i>	<i>Frames per projection</i>	<i>Exposure time per frame (ms)</i>	<i>Approx. total time per acquisition (min)</i>
<i>Acanella arbuscula</i>	Complete structure	Circular (360°) CT	50	50	80	12	2501	4	89	15
	Central branch	Circular (360°) CT	15	15	80	8.9	2001	4	125	17
<i>Keratoisis</i> sp.	Complete structure	Circular (360°) CT	15	15	80	8.9	3501	4	354	83

309

310

311 References

- 312 1 Robinson, L. F. *et al.* The geochemistry of deep-sea coral skeletons: A review of vital
313 effects and applications for palaeoceanography. *Deep Sea Res. Part I Oceanogr.*
314 *Res.* **99**, 184-198 (2014).
- 315 2 Thresher, R. E., Fallon, S. J. & Townsend, A. T. A “core-top” screen for trace element
316 proxies of environmental conditions and growth rates in the calcite skeletons of
317 bamboo corals (*Isididae*). *Geochim. Cosmochim. Acta* **193**, 75-99 (2016).
- 318 3 Pierrejean, M. *et al.* Influence of Deep-Water Corals and Sponge Gardens on
319 Infaunal Community Composition and Ecosystem Functioning in the Eastern
320 Canadian Arctic. *Front. Mar. Sci.* **7** (2020).
- 321 4 Hill, T. M. *et al.* Temperature and vital effect controls on bamboo coral (*Isididae*)
322 isotope geochemistry: A test of the “lines method”. *Geochem. Geophys. Geosystems*
323 **12**, Q04008 (2011).
- 324 5 Farmer, J. R., Robinson, L. F. & Honisch, B. Growth rate determinations from
325 radiocarbon in bamboo corals (genus *Keratoisis*). *Deep-Sea Res. Part I-Oceanogr.*
326 *Res. Pap.* **105**, 26-40 (2015).
- 327 6 Tambutté, E. *et al.* Morphological plasticity of the coral skeleton under CO₂-driven
328 seawater acidification. *Nat. Commun.* **6**, 7368 (2015).
- 329 7 Li, Y. *et al.* The 3D Reconstruction of Pocillopora Colony Sheds Light on the Growth
330 Pattern of This Reef-Building Coral. *iScience* **23**, 101069 (2020).
- 331 8 Alvarez-Filip, L., Côté, I. M., Gill, J. A., Watkinson, A. R. & Dulvy, N. K. Region-wide
332 temporal and spatial variation in Caribbean reef architecture: is coral cover the whole
333 story? *Glob. Change Biol* **17**, 2470-2477 (2011).
- 334 9 Odum, H. T. & Odum, E. P. Trophic structure and productivity of a windward coral
335 reef community on Eniwetok Atoll. *Ecol Monogr.* **25**, 291-320 (1995).
- 336 10 Li, Y. *et al.* Micro-CT reconstruction reveals the colony pattern regulations of four
337 dominant reef-building corals. *Ecol. Evol.* **11**, 16266-16279 (2021).
- 338 11 Urushihara, Y., Hasegawa, H. & Iwasaki, N. X-ray micro-CT observation of the apical
339 skeleton of Japanese white coral *Corallium konojoi*. *J. Exp. Mar. Biol.* **475**, 124-128
340 (2016).
- 341 12 Gutiérrez-Heredia, L., D'Helft, C. & Reynaud, E. G. Simple methods for interactive 3D
342 modeling, measurements, and digital databases of coral skeletons. *Limnol.*
343 *Oceanogr. Meth.* **13**, 178-193 (2015).
- 344 13 Crook, E. D., Cohen, A. L., Rebolledo-Vieyra, M., Hernandez, L. & Paytan, A.
345 Reduced calcification and lack of acclimatization by coral colonies growing in areas of
346 persistent natural acidification. *Proc. Natl. Acad. Sci. U.S.A.* **110**, 11044-11049
347 (2013).
- 348 14 Corbera, G. *et al.* Glacio-eustatic variations and sapropel events as main controls on
349 the Middle Pleistocene-Holocene evolution of the Cabliers Coral Mound Province (W
350 Mediterranean). *Quat Sci Rev.* **253**, 106783 (2021).
- 351 15 Morales Pinzon, A. *et al.* A semi-automatic method to extract canal pathways in 3D
352 micro-CT images of Octocorals. *PLoS One* **9**, e85557 (2014).
- 353 16 Mollica, N. R. *et al.* Skeletal records of bleaching reveal different thermal thresholds
354 of Pacific coral reef assemblages. *Coral Reefs* **38**, 743-757 (2019)
- 355 17 Reznikov, N., Buss, D. J., Provencher, B., McKee, M. D. & Piche, N. Deep learning
356 for 3D imaging and image analysis in biomineralization research. *J. Struct. Biol.* **212**,
357 107598 (2020).

- 358 18 Lu, X. Z., Lai, C. P. & Chan, L. C. Novel design of a coral-like open-cell porous
359 degradable magnesium implant for orthopaedic application. *Mater. Des.* **188**, 108474
360 (2020).
- 361 19 Chen, D. A., Ross, B. E. & Klotz, L. E. Lessons from a Coral Reef: Biomimicry for
362 Structural Engineers. *J. Struct. Eng.* **141**, (2015).
- 363 20 DeCarlo, T. M. & Cohen, A. L. Dissepiments, density bands and signatures of thermal
364 stress in Porites skeletons. *Coral Reefs* **36**, 749-761 (2017).
- 365 21 DeCarlo T.M., and Cohen A.L. coralCT: software tool to analyze computerized
366 tomography (CT) scans of coral skeletal cores for calcification and bioerosion rates.
367 doi:10.5281/zenodo.3402343. (2019).
- 368 22 Fordyce, A. J. *et al.* Understanding decay in marine calcifiers: Micro-CT analysis of
369 skeletal structures provides insight into the impacts of a changing climate in marine
370 ecosystems. *Methods Ecol.* **11**, 1021-1041 (2020).
- 371 23 Williams T.J. *et al.* Geochemical proxies for deep-sea temperature and nutrient
372 content in cold-water bamboo corals. *Chem. Geol.* **654**, 122053 (2024).
- 373 24 Li, Y., Liao, X., He, C. & Lu, Z. Calcium Transport along the Axial Canal in Acropora.
374 *Diversity* **13**, 407 (2021).
- 375 25 Geiger, F. *et al.* VEGF producing bone marrow stromal cells (BMSC) enhance
376 vascularization and resorption of a natural coral bone substitute. *Bone* **41**, 516-522
377 (2007).
- 378 26 Schindelin, J. *et al.* Fiji: an open-source platform for biological-image analysis. *Nat.*
379 *Methods* **9**, 676-682 (2012).
- 380 27 Gilkinson, K., & Edinger, E. (Eds.) The ecology of deep-sea corals of Newfoundland
381 and Labrador waters: biogeography, life history, biogeochemistry, and relation to
382 fishes. *Can. Tech. Rep. Fish. Aquat. Sci.* **2830**. vi + 136 (2009).
- 383 28 Hiltz, E., Fuller, S. D. & Mitchell, J. Disko Fan Conservation Area: a Canadian case
384 study. *Parks* **24**, 17-30 (2018).
- 385 29 Roff, J. C. *et al.* Marine Ecological Conservation for the Canadian Eastern Arctic
386 (MECCEA) – a Systematic Planning Approach for Identifying Priority Areas for
387 Conservation. 281 + xxii (2020).
- 388 30 Fuller, S. D., Perez, F. J. M., Wareham, V. & Kenchington, E. Vulnerable Marine
389 Ecosystems Dominated by Deep-Water Corals and Sponges in the NAFO
390 Convention Area. Report No. N5524, (Northwest Atlantic Fisheries Organization,
391 2008).
- 392 31 Neves, B. d. M. *et al.* Deep-water bamboo coral forests in a muddy Arctic
393 environment. *Mar. Biodivers.* **45**, 867-871 (2014).
- 394 32 Johannes, R. E. & Wiebe, W. J. Method for determination of coral tissue biomass and
395 composition. *Limnol. Oceanogr.* **15**, 822-824 (1970).
- 396 33 Katsamenis, O. L. *et al.* A high-throughput 3D X-ray histology facility for biomedical
397 research and preclinical applications. *Wellcome Open Res.* **8**, 366 (2023).
- 398 34 Katsamenis, O. L., Basford, P. J. & Robinson, S. K. muvis-tomography/XRH-
399 processing-toolbox (v0.2). *Zenodo* <https://doi.org/10.5281/zenodo.11148752> (2023).
- 400 35 Williams, T. J. *et al.* High-resolution three-dimensional images of deep-sea bamboo
401 corals *Acanella arbuscula* and *Keratoisis* sp. collected in the Baffin Bay and Davis
402 Strait during the CCGS Amundsen expedition in 2021 (Version 1.0) [Data set]. NERC
403 EDS UK Polar Data Centre. doi:10.5285/76534D05-BA4E-47B7-9685-
404 0A8C88404EF2 (2023).

- 405 36 Carmignato, S., Pierobon, A., Rampazzo, P., Parisatto, M. & Savio, E. CT for
406 Industrial Metrology – Accuracy and Structural Resolution of CT Dimensional
407 Measurements. *Nondestruct. Test. Evaluation* **17**(12) (2012).
- 408 37 Yushkevich P. A. & Gerig, G. ITK-SNAP: An Intractive Medical Image Segmentation
409 Tool to Meet the Need for Expert-Guided Segmentation of Complex Medical Images.
410 *IEEE Pulse*, **8**(4), 54-57 (2017).